RESEARCH ARTICLE OPEN ACCESS

Flight Attitude Controller Using Dynamic Inversion Theory with Stability Margin Guarantee

Kento Shirakata*, Koichi Yonemoto*, Takahiro Fujikawa*
**Department of Mechanical and Control Engineering, Kyushu Institute of Technology, Japan*
Corresponding Author: Kento Shirakata

ABSTRACT
In order to realize reusable launch vehicle, flight attitude control system is important. Dynamic inversion (DI) theory is known well as nonlinear control theory. DI theory can cancel the nonlinear dynamics and linearize the input and output maps. Therefore, closed loop analysis through flight trajectory becomes easier than other control systems, e.g. gain tuning method. When we use DI theory, we must know certain dynamics models. However, since modeling errors necessarily arise, ensuring robustness is important. Even using DI theory, stability margins cannot be uniquely determined because the loop is opened when we calculate stability margins. In this paper, the authors propose the stability margin guaranteeing method for flight control system using DI theory.In this article the authors propose the new evaluation function for guaranteeing required stability margin. By onboard design variable tuning, all stability margins become larger than required ones.
Keywords–stability margin, dynamic inversion, flight controller, nonlinear control

DATE OF SUBMISSION: 20-12-2018 DATE OF ACCEPTANCE: 04-01-2019

I. INTRODUCTION

In recent years, reusable launch vehicles have been researched and developed around the world. If the reusable vehicles are realized, they are expected in reducing the launch cost and promoting space development. Advantages of using winged rockets for space transportation are reusability, operability, and abort capability. The dynamics of the winged rocket are highly nonlinear due to the wide flight envelope ranging between subsonic and hypersonic speed and has aerodynamically nonlinear parameters. Therefore, a nonlinear flight attitude control system that can adapt to various flight conditions is important for realizing winged reusable space transportation system.

Dynamic Inversion (DI) theory is one of nonlinear control theories that can handlethe nonlinear dynamics by state matrix feedback and makes a desired closed loop system to linear dynamics [1],[2]. It requires the r -order differentiation in DI calculation where r is the relative degree between controlled variables and control inputs. Therefore, designing a control system for a large r -order becomes complicated. Researchers have been proposing various concepts to reduce these complications by separating the complex system into smaller simple subsystems[3]-[6]. In these approaches, “Hierarchical DI theory”, proposed by Yamasaki, H. is superior in terms of separation criteria for a complex system and evaluation of the closed loop system’s responses [6].

For a nonlinear system, stability margins (gain margin and phase margin) are evaluated by locally linearized transfer function calculated by Taylor expansion of nonlinear system in steady state space. In case of hierarchical DI theory, the evaluation method employed is same for conventional linear control systems and the nonlinear dynamics is not linearized if the feedback loop is open.

In order to satisfy the desired stability margin requirement, control gain tuning method using sensitivity function are proposed in linear control systems [7]-[9]. This approach is applicable only if the poles of the open loop system are not unstable. However for a traditional aircraft or winged launch vehicles, unstable low frequency poles of the open loop system are allowed. Therefore, it is necessary to developan approach for a system with unstable poles.

In this research, the authors expand control gain tuning method using sensitivity function to the unstable open loop system, and incorporate this expanded method into hierarchical DI theory to realize the flight control system with stability margin guarantee.

II. HIERARCHAL DI THEORY

2.1 DI theory

This theory cancels the nonlinear dynamics by state matrix feedback and makes the closed loop system to desired linear dynamics. There are l states, m inputs, and m outputs nonlinear dynamics expressed in Eq.(1),

$$\dot{\boldsymbol{x}} = \boldsymbol{f}(\boldsymbol{x}) + \boldsymbol{g}(\boldsymbol{x})\boldsymbol{u} \quad \boldsymbol{y} = \boldsymbol{h}(\boldsymbol{x}) \tag{1}$$

where $\boldsymbol{x} \in {}^{l}$ is state vector, $\boldsymbol{y} \in {}^{m}$ is controlled variables vector, and $\boldsymbol{u} \in {}^{m}$ is control input vector. In addition, the coefficient matrixes are expressed in Eq.(2).

$$\boldsymbol{f}(\boldsymbol{x}) = \begin{bmatrix} f_1(\boldsymbol{x}) \\ \vdots \\ f_l(\boldsymbol{x}) \end{bmatrix} \quad \boldsymbol{g}(\boldsymbol{x}) = \begin{bmatrix} g_{1,1}(\boldsymbol{x}) & \cdots & g_{1,m}(\boldsymbol{x}) \\ \vdots & \ddots & \vdots \\ g_{l,1}(\boldsymbol{x}) & \cdots & g_{l,m}(\boldsymbol{x}) \end{bmatrix} \quad \boldsymbol{h}(\boldsymbol{x}) = \begin{bmatrix} h_1(\boldsymbol{x}) \\ \vdots \\ h_n(\boldsymbol{x}) \end{bmatrix} \tag{2}$$

Let $L_f{}^r \boldsymbol{h}(\boldsymbol{x})$ be the Lie derivative whose definition is expressed in Eq.(2),

$$L_f \boldsymbol{h}(\boldsymbol{x}) = \frac{d\boldsymbol{h}(\boldsymbol{x})}{dt} \boldsymbol{f}(\boldsymbol{x}) = \sum_{i=1}^{l} \frac{\partial \boldsymbol{h}(\boldsymbol{x})}{\partial x_i} f_i(\boldsymbol{x}) \tag{2}$$

whenthe relative degree of the system is r -order, the r order derivative of $\boldsymbol{y}$ is expressed in Eq (3).

$$\boldsymbol{y}^{(r)} = L_f{}^r \boldsymbol{h}(\boldsymbol{x}) + \left(L_g L_f{}^{r-1} \boldsymbol{h}(\boldsymbol{x})\right)\boldsymbol{u} \tag{3}$$

Therefore, a control input vector is given by the following equation.

$$\boldsymbol{u} = \left(L_g L_f{}^{r-1} \boldsymbol{h}(\boldsymbol{x})\right)^{-1} \left(\boldsymbol{y}^{(r)} - L_f{}^r \boldsymbol{h}(\boldsymbol{x})\right) \tag{4}$$

Now, by introducing pseudo input vector $\boldsymbol{v}$, definedbyEq(5)

$$\boldsymbol{v} = \boldsymbol{y}^{(r)} \tag{5}$$

control input command vector $\boldsymbol{u}_{com}$ can be calculated by Eq(6).

$$\boldsymbol{u}_{com} = \left(L_g L_f{}^{r-1} \boldsymbol{h}(\boldsymbol{x})\right)^{-1} \left(\boldsymbol{v} - L_f{}^r \boldsymbol{h}(\boldsymbol{x})\right) \tag{6}$$

When $\boldsymbol{v}$ is designed as a general linear response such as (7),

$$\boldsymbol{v} = -\left(\boldsymbol{K}_{r-1}\boldsymbol{y}^{(r-1)} + \boldsymbol{K}_{r-2}\boldsymbol{y}^{(r-2)} + \ldots + \boldsymbol{K}_0 \boldsymbol{y}\right) + \boldsymbol{K}_0 \boldsymbol{y}_{com} \tag{7}$$

the closed loop transfer function is expressed by(8),

$$\boldsymbol{P}(s) = \left(s^r \boldsymbol{I} + \boldsymbol{K}_{r-1} s^{r-1} + \boldsymbol{K}_{r-2} s^{r-2} + \ldots + \boldsymbol{K}_0\right)^{-1} \boldsymbol{K}_0 \tag{8}$$

where

$$\boldsymbol{K}_i = \mathrm{diag}\left(K_1, K_2, \ldots, K_n\right) \quad \left(i = 0, 1, \ldots, r-1\right) \tag{9}$$

and $\boldsymbol{I}$ is identity matrix of size n and $K_j \left(j = 0, 1, \ldots, n\right)$ are design variables.

2.2 Hierarchal DI theory

Hierarchal DI theory [6] is a method to reduce the complication when a control system is designed by using DI, especially when the relative degree of the system is large. When the nonlinear system is expressed by block-strict-feedback form consisting of hierarchal p instead of affine system proposed in previousresearches [6] is shown in Eq. (11).

$$\begin{bmatrix} \dot{\boldsymbol{x}}_1 \\ \vdots \\ \dot{\boldsymbol{x}}_i \\ \vdots \\ \dot{\boldsymbol{x}}_p \end{bmatrix} = \begin{bmatrix} \boldsymbol{F}_1(\boldsymbol{x}_1) \\ \vdots \\ \boldsymbol{F}_i(\boldsymbol{x}_1, \ldots, \boldsymbol{x}_i) \\ \vdots \\ \boldsymbol{F}_p(\boldsymbol{x}_1, \ldots, \boldsymbol{x}_p) \end{bmatrix} + \begin{bmatrix} \boldsymbol{G}_1(\boldsymbol{x}_1)\boldsymbol{y}_2 \\ \vdots \\ \boldsymbol{G}_1(\boldsymbol{x}_1, \ldots, \boldsymbol{x}_i)\boldsymbol{y}_{i+1} \\ \vdots \\ \boldsymbol{G}_1(\boldsymbol{x}_1, \ldots, \boldsymbol{x}_p)\boldsymbol{u} \end{bmatrix} \quad \begin{bmatrix} \boldsymbol{y}_1 \\ \vdots \\ \boldsymbol{y}_i \\ \vdots \\ \boldsymbol{y}_p \end{bmatrix} = \begin{bmatrix} \boldsymbol{h}_1(\boldsymbol{x}_1) \\ \vdots \\ \boldsymbol{h}_i(\boldsymbol{x}_i) \\ \vdots \\ \boldsymbol{h}_p(\boldsymbol{x}_p) \end{bmatrix} \tag{11}$$

where

$$\boldsymbol{F}_i(\boldsymbol{x}_1, \ldots, \boldsymbol{x}_i) = \begin{bmatrix} f_{i,1}(\boldsymbol{x}_1, \ldots, \boldsymbol{x}_i) \\ \vdots \\ f_{i,l_i}(\boldsymbol{x}_1, \ldots, \boldsymbol{x}_i) \end{bmatrix} \quad \boldsymbol{G}_i(\boldsymbol{x}_1, \ldots, \boldsymbol{x}_i) = \begin{bmatrix} \boldsymbol{g}_{i,1}(\boldsymbol{x}_1, \ldots, \boldsymbol{x}_i) \\ \vdots \\ \boldsymbol{g}_{i,l_i}(\boldsymbol{x}_1, \ldots, \boldsymbol{x}_i) \end{bmatrix} \quad \boldsymbol{g}_{i,k}(\boldsymbol{x}_1, \ldots, \boldsymbol{x}_i) = \begin{bmatrix} g_{i,k,1}(\boldsymbol{x}_1, \ldots, \boldsymbol{x}_i) \\ \vdots \\ g_{i,k,m_i}(\boldsymbol{x}_1, \ldots, \boldsymbol{x}_i) \end{bmatrix}^T \tag{12}$$

and i th subsystem has l_i states, m_i control inputs, and m_i outputs. The i th subsystem is said to have relative degree r_i as expressed below.

$$L_{G_i} L_{F_i}^{r_i - 1} \boldsymbol{h}_i(\boldsymbol{x}_i) \neq 0 \tag{10}$$

Therefore, control input commands for each subsystems are defined as following equations,

$$\begin{aligned} y_{com_2} &= \left(L_{G_1} L_{F_1}^{r_1-1} h_1(x_1)\right)^{-1} \\ &\quad \left(v_1 - L_{F_1}^{r_1} h_1(x_1)\right) \\ &\vdots \\ y_{com_{i+1}} &= \left(L_{G_i} L_{F_i}^{r_i-1} h_i(x_i)\right)^{-1} \\ &\quad \left(v_i - L_{F_i}^{r_i} h_i(x_i)\right) \\ &\vdots \\ y_{com_p} &= \left(L_{G_{p-1}} L_{F_{p-1}}^{r_{p-1}-1} h_{p-1}(x_{p-1})\right)^{-1} \\ &\quad \left(v_{p-1} - L_{F_{p-1}}^{r_{p-1}} h_{p-1}(x_{p-1})\right) \\ u_{com} &= \left(L_{G_p} L_{F_p}^{r_p-1} h_p(x_p)\right)^{-1} \\ &\quad \left(v_p - L_{F_p}^{r_p} h_p(x_p)\right) \end{aligned} \tag{14}$$

where $v_i\left(i=1,\dots,p\right)$ is pseudo input vector in each subsystem, and these are defined by following linear feedback law in order to realize desired linear responses.

$$\begin{aligned} v_i &= -\left(K_{i,r_i-1} y_i^{(r-1)} + \dots + K_{i,0} y_i\right) \\ &\quad + K_{i,0} y_{com_i} \end{aligned} \tag{11}$$

Therefore, the closed loop transfer function of the p th subsystem is expressed by (12). I is identity matrix of size m_p.

$$\begin{aligned} P_p(s) &= \left(s^{r_p} I + K_{p,r_p-1} s^{r_p-1} + \right. \\ &\quad \left. K_{p,r_p-2} s^{r_p-2} + \dots + K_{p,0}\right)^{-1} K_{p,0} \end{aligned} \tag{12}$$

And, the $p-1$ th subsystem expressed by (13).

$$\begin{aligned} y_{p-1}^{(r_{p-1})} &= L_{F_{p-1}}^{(r_{p-1})} h(x_{p-1}) \\ &\quad + \left(L_{G_{p-1}} L_{F_{p-1}}^{(r_{p-1}-1)} h(x_{p-1})\right) y_p \end{aligned} \tag{13}$$

From (12) and (13), the $p-1$ th subsystem is rewritten by (14).

$$\begin{aligned} y_{p-1}^{(r_{p-1})} &= L_{F_{p-1}}^{(r_{p-1})} h(x_{p-1}) \\ &\quad + \left(L_{G_{p-1}} L_{F_{p-1}}^{(r_{p-1}-1)} h(x_{p-1})\right) \\ &\quad P_p(s) y_{com_p} \end{aligned} \tag{14}$$

If $P_p(s)$ is scalar matrix, $p-1$ th subsystem is expressed by (15)using**Error! Reference source not found.** and (14).

$$\begin{aligned} y_{p-1}^{(r_{p-1})} &= \left(I - P_p(s)\right) L_{F_{p-1}}^{(r_{p-1})} h(x_{p-1}) \\ &\quad + P_p(s) v_{p-1} \end{aligned} \tag{15}$$

This subsystem can be separated into linear term (TF_L) and nonlinear term (TF_{NL}).

$$\begin{aligned} TF_L &= P_p(s) v_{p-1} \\ TF_{NL} &= \left(I - P_p(s)\right) L_{F_{p-1}}^{(r_{p-1})} h(x_{p-1}) \end{aligned} \tag{16}$$

When p th subsystem has very fast response,

$$\begin{aligned} P_p(s) &\approx I \\ \left(I - P_p(s)\right) &\approx 0 \end{aligned} \tag{17}$$

Then,(15) is approximated to linear system as (18).

$$y_{p-1}^{(r_{p-1})} \approx P_p(s) v_{p-1} \tag{18}$$

Therefore, closed loop transfer function is expressed by (19).

$$\begin{aligned} P_{p-1}(s) &= \left\{s^{r_{p-1}} I + P_p(s)\left(K_{p-1,r_{p-1}-1} s^{r_{p-1}-1}\right.\right. \\ &\quad \left.\left. + \dots + K_{p-1,0} y_{p-1}\right)\right\}^{-1} \\ &\quad P_p(s) K_{p-1,0} y_{com_{p-1}} \end{aligned} \tag{19}$$

For this result, closed loop transfer function for i thsubsystem is given by pseudo inputs for i th subsystem and transfer function of $i-1$ th subsystem. In previous research, this closed loop transfer function is called Linearized Approximation Transfer Functions (LATF) [6]. LATF of each subsystems is given by **Error! Reference source not found.**.

$$\begin{aligned} P_1 &= \left\{s^{r_1} I + P_2\left(K_{1,r_1-1} s^{r_1-1}\right.\right. \\ &\quad \left.\left. + \dots + K_{1,0}\right)\right\}^{-1} P_1 K_{2,0} \\ &\vdots \\ P_i &= \left\{s^{r_i} I + P_{i+1}\left(K_{i,r_i-1} s^{r_i-1}\right.\right. \\ &\quad \left.\left. + \dots + K_{i,0}\right)\right\}^{-1} P_{i+1} K_{i,0} \\ &\vdots \\ P_{p-1}(s) &= \left\{s^{r_{p-1}} I + P_p(s)\right. \\ &\quad \left(K_{p-1,r_{p-1}-1} s^{r_{p-1}-1}\right. \\ &\quad \left.\left. + \dots + K_{p-1,0}\right)\right\}^{-1} \\ &\quad P_p(s) K_{p-1,0} \\ P_p(s) &= \left(s^{r_p} I + K_{p,r_p-1} s^{r_p-1}\right. \\ &\quad \left. K_{p,r_p-2} s^{r_p-2} + \dots + K_{p,0}\right)^{-1} K_{p,0} \end{aligned} \tag{24}$$

III. GAIN TUNING METHOD WITH STABILITY MARGIN GUARANTEE

3.1 Using sensitivity function

In previousresearches,methods that guarantee the desired stability margins requirements using sensitivity function are studied [7]. On nyquist diagram, inverse absolute value of sensitivity function is expressed by the distance between the point (-1,0) and open loop transfer function on a complex plane. This distance expresses the stability, therefore stability margins are guaranteed if maximum sensitivity function (often called M_s) is smaller than desired M_s which is calculated by desired gain margin and phase margin.

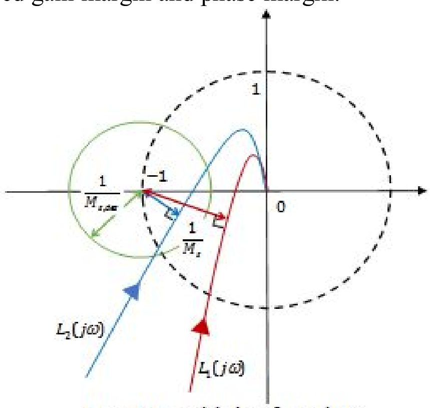

Fig. 1 Sensitivity function

In **Error! Reference source not found.**, green solid line circle represents the desired stability margins requirements. $L_1(j\omega)$ (red solid line) does not enter the circle, therefore desired stability margins are guaranteed. $L_2(j\omega)$ (blue solid line) enters the circle therefore desired stability margins are not guaranteed. The relation amongan open loop system ($L(j\omega)$), a sensitivity function ($S(j\omega)$), stability margins (g_m ,ϕ_m), and M_s , as follows.

$$S(j\omega) = \left(1 + L(j\omega)\right)^{-1} \tag{20}$$

$$M_s = \max_{\omega} \left|S(j\omega)\right| \tag{21}$$

$$g_m \geq \frac{M_s}{M_s - 1}$$
$$\phi_m \geq 2\sin^{-1}\frac{1}{2M_s} \tag{22}$$

Then, desired M_s is derived by desired stability margins requirements. Where $g_{m,des}$ is a desired gain margin in magnitude and $\phi_{m,des}$ is a desired phase margin in radian.

$$M_{s,g,des} = \frac{g_{m,des}}{g_{m,des} - 1}$$
$$M_{s,p,des} = \frac{1}{2\sin\left(\phi_{m,des}/2\right)} \tag{23}$$
$$M_{s,des} = \min\left(M_{s,g,des}, M_{s,p,des}\right)$$

This method is applicable for anopen loop system which doesnot have positive poles, therefore it cannotbe appliedto a system which has multiple phase crossovers. Open loop systems of winged vehicles are often allowed that they have unstable poles at low frequency. In the next section, method which expands guaranteeing stability margins for a system with multiple phase crossovers are explained.

3.2 Expanded gain tuning method for multiple phase crossovers

This is a case for an open loop system whichhas multiple phase crossovers, meaning there are multiple gain margins. For example, the system has $g_{m,1}$ and $g_{m,2}$ where $g_{m,2}$ is anegative gain margin in dB.

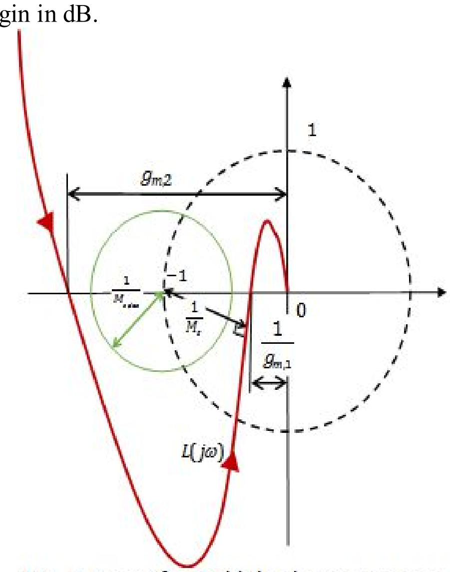

Fig. 2 A case for multiple phase crossovers

Previous methods [7]-[9]cannot consider negative gain margins. Now the authors propose a new circle condition to consider negative gain margins.

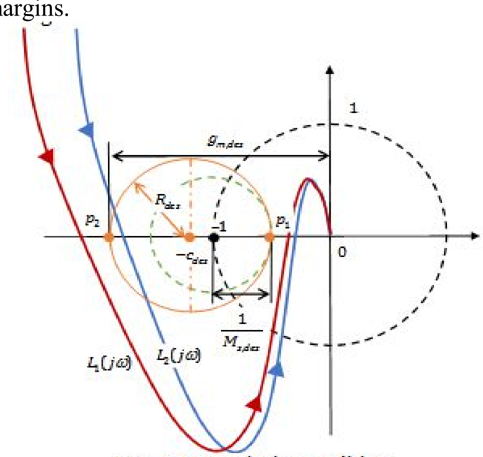

Fig. 3 New circle condition

In **Error! Reference source not found.**, new circle is shown by orange-colored solid line and the previous circle is shown by green dotted line.

$L_1(j\omega)$ (red solid line) does not enter the circle, therefore desired positive and negative stability margins are guaranteed. The way of definingof p_1 is same as the previous methods (23) and (24). p_2 is defined by desired gain margin in magnitude (25). Thus,center $(-c_{des},0)$ and radius R_{des} of the new circle are expressed in (26) and (27).

$$p_1 = -1 + \frac{1}{M_{s,des}} \tag{24}$$

$$p_2 = -g_{m,des} \tag{25}$$

$$-c_{des} = \frac{p_1 + p_2}{2} \tag{26}$$

$$R_{des} = \frac{p_1 - p_2}{2} \tag{27}$$

When the open loop transfer function doesnot enter the circle, the system is guaranteed with a desired phase margin and gain margin. Then, the authors introduced an evaluation function $E(j\omega)$ as shown in(28); it represents the distance between the point $(-c_{des},0)$ and an open loop $L(j\omega)$. Therefore the condition that guarantees a system with a desired stability margins is expressed in(29).

$$E(j\omega) = \left| \frac{1}{L(j\omega) + c_{des}} \right| \tag{28}$$

$$\max_{\omega}\left(E(j\omega)\right) \geq \frac{1}{R_{des}} \tag{29}$$

Stability margins evaluation methodfor a system with multiple gain crossovers or multiple phase crossovers is studied [10]. He proposed that, a phase margin and gain margin (unit : dB) should be evaluated by minimum one in absolute value. Maximum evaluation function means minimum distance between $(-c_{des},0)$ and $L(j\omega)$ thus, it guarantees a minimum gain margin and phase margin in absolute value which are bigger than the desired margins.

IV. APPLICATION TO WINGED ROCKET

In this section, the winged rocket attitude control system using hierarchal DI theory and pseudo input gain matrices ($\boldsymbol{K}$ in (11)) which are tuned by expanded method for stability margin introduced in the previous section are considered. The winged rocket“WIRES” (WInged REusable Sounding rocket) which has two elevons and rudders forattitude control are shown in Fig. 4 and the control system diagram is shown in Fig.5. This rocket is an experimental winged rocket developed in Kyushu Institute of Technology [11]-[13]. This flight dynamics is based on general airplane [14].

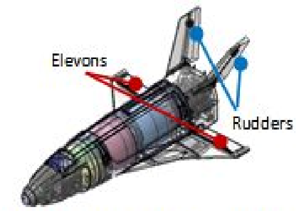

Fig. 4 WIRES rocket with control surfaces

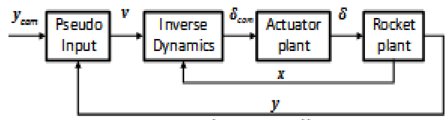

Fig. 5 Control system diagram

Table 1 State variables

V_c	[m/s]	True air speed (TAS)
α	[rad]	Angle of attack (AoA)
β	[rad]	Side slip angle (SSA)
P	[rad/s]	Roll angular velocity
Q	[rad/s]	Pitch angular velocity
R	[rad/s]	Yaw angular velocity
ϕ	[rad]	Roll angle
θ	[rad]	Pitch angle

Table 2 Control input variables and pseud input variables

δ_a	[rad]	Aileron angle
δ_e	[rad]	Elevator angle
δ_r	[rad]	Rudder angle
v_α	[rad/s^2]	AoA pseudo input
v_β	[rad/s^2]	SSA pseudo input
v_ϕ	[rad/s^2]	Roll pseudo input

Each vectors are defined by following equation.

$$\boldsymbol{x} = \begin{bmatrix} V_c & \alpha & \beta & P & Q & R & \phi & \theta \end{bmatrix}^T \tag{30}$$

$$\boldsymbol{y} = \begin{bmatrix} \alpha & \beta & \phi \end{bmatrix}^T \tag{31}$$

$$\boldsymbol{\delta} = \begin{bmatrix} \delta_a & \delta_e & \delta_r \end{bmatrix}^T \tag{32}$$

$$\boldsymbol{v} = \begin{bmatrix} v_\alpha & v_\beta & v_\phi \end{bmatrix}^T \tag{33}$$

4.1 Plant dynamics model

Now, let’s consider the followingtwo-level hierarchical system for the winged rocket. First subsystem is for the flight dynamics and second subsystem is for the actuator dynamics.

$$\begin{bmatrix} \dot{\boldsymbol{x}} \\ \dot{\boldsymbol{x}}_\delta \end{bmatrix} = \begin{bmatrix} \boldsymbol{F}_1(\boldsymbol{x}) \\ \boldsymbol{F}_2(\boldsymbol{x}_\delta) \end{bmatrix} + \begin{bmatrix} \boldsymbol{G}_1(\boldsymbol{x})\boldsymbol{\delta} \\ \boldsymbol{G}_2(\boldsymbol{x}_\delta)\boldsymbol{\delta}_{com} \end{bmatrix}$$
$$\begin{bmatrix} \boldsymbol{y} \\ \boldsymbol{\delta} \end{bmatrix} = \begin{bmatrix} \boldsymbol{h}_1(\boldsymbol{x}) \\ \boldsymbol{h}_2(\boldsymbol{x}_\delta) \end{bmatrix} \tag{34}$$

Both the subsystems have related degree 2, and actuator dynamics are linear and can be expressed by a scalar matrix as following.

$$\ddot{\boldsymbol{\delta}} = -\omega_{act}{}^2 \boldsymbol{I}\boldsymbol{\delta} - 2\zeta_{act}\omega_{act}\boldsymbol{I}\dot{\boldsymbol{\delta}} + \omega_{act}{}^2 \boldsymbol{I}\boldsymbol{\delta}_{com} \tag{35}$$

$$\boldsymbol{P}_{act}(s) = \frac{\omega_{act}{}^2}{s^2 + 2\zeta_{act}\omega_{act}s + \omega_{act}{}^2}\boldsymbol{I} \tag{36}$$

4.2 Application of hierarchal DI theory to winged rocket

Thesecond order derivative of controlled vector is as follows.

$$\ddot{\boldsymbol{y}} = L_{F_1}^2 \boldsymbol{h}_1(\boldsymbol{x}) + L_{G_1} L_{F_1} \boldsymbol{h}_1(\boldsymbol{x})\boldsymbol{\delta} \tag{37}$$

Therefore, the control surface commands (control input vector commands) are calculated by solving inverse dynamics with pseudo inputs as shown in (38).

$$\boldsymbol{\delta}_{com} = \left(L_{G_1} L_{F_1} \boldsymbol{h}_1(\boldsymbol{x})\right)^{-1} \left(\boldsymbol{v} - L_{F_1}^2 \boldsymbol{h}_1(\boldsymbol{x})\right) \tag{38}$$

From (36), since actuator dynamics is a scalar matrix, linearized approximation transfer function matrix is shown in(39).

$$\boldsymbol{P}_{LATF} = \left(s^2\boldsymbol{I} + \boldsymbol{P}_{act}\boldsymbol{K}_D s + \boldsymbol{P}_{act}\boldsymbol{K}_P\right)^{-1} \boldsymbol{P}_{act}\boldsymbol{K}_P \tag{39}$$

In previous research [6], PD gain matrices ($\boldsymbol{K}_P, \boldsymbol{K}_D$) are selected from the desired second order response; damping ratio ζ_{des} [-] and frequency ω_{des} [rad/s].

$$K_{P_i} = \omega_{des,i}{}^2, K_{D_i} = 2\zeta_{des,i}\omega_{des,i}$$
$$(i = \alpha, \beta, \phi)$$
$$\boldsymbol{K}_j = \mathrm{diag}\left(K_{j_\alpha}, K_{j_\beta}, K_{j_\phi}\right) \tag{40}$$
$$(j = P, D)$$

This article shows how to tune ω_{des} by guaranteeing stability margins, and the authors call ω_{des} as desired frequency.

4.3 Application of gain tuning method to winged rocket attitude control using hierarchal DI theory

First, we derive an open loop system for a locally linearized winged rocket control system using DI theory. The locally linearized model of rocket dynamics and DI controller are given in(41) and (42).

$$\begin{aligned}
\Delta\dot{\boldsymbol{x}} &= \frac{\partial}{\partial \boldsymbol{x}}\left(\boldsymbol{F}_1(\boldsymbol{x}) + \boldsymbol{G}_1(\boldsymbol{x})\boldsymbol{\delta}\right)\Big|_{\boldsymbol{x}=\boldsymbol{x}_0, \boldsymbol{\delta}=\boldsymbol{\delta}_0} \Delta\boldsymbol{x} \\
&+ \frac{\partial}{\partial \boldsymbol{\delta}}\left(\boldsymbol{F}_1(\boldsymbol{x}) + \boldsymbol{G}_1(\boldsymbol{x})\boldsymbol{\delta}\right)\Big|_{\boldsymbol{x}=\boldsymbol{x}_0, \boldsymbol{\delta}=\boldsymbol{\delta}_0} \Delta\boldsymbol{\delta} \\
&= \frac{\partial}{\partial \boldsymbol{x}}\left(\boldsymbol{F}_1(\boldsymbol{x}) + \boldsymbol{G}_1(\boldsymbol{x})\boldsymbol{\delta}\right)\Big|_{\boldsymbol{x}=\boldsymbol{x}_0, \boldsymbol{\delta}=\boldsymbol{\delta}_0} \Delta\boldsymbol{x} \\
&+ \boldsymbol{G}_1(\boldsymbol{x})\Big|_{\boldsymbol{x}=\boldsymbol{x}_0} \Delta\boldsymbol{\delta}
\end{aligned} \tag{41}$$
$$\begin{aligned}
\Delta\boldsymbol{x} &= \left(s\boldsymbol{I} - \frac{\partial}{\partial \boldsymbol{x}}\left(\boldsymbol{F}_1(\boldsymbol{x}) + \boldsymbol{G}_1(\boldsymbol{x})\boldsymbol{\delta}\right)\Big|_{\boldsymbol{x}=\boldsymbol{x}_0, \boldsymbol{\delta}=\boldsymbol{\delta}_0}\right)^{-1} \\
&\quad \boldsymbol{G}_1(\boldsymbol{x})\Big|_{\boldsymbol{x}=\boldsymbol{x}_0} \Delta\boldsymbol{\delta} \\
&= \boldsymbol{P}_{FLT}(s, \boldsymbol{x}_0, \boldsymbol{\delta}_0)\Delta\boldsymbol{\delta}
\end{aligned}$$

$$\begin{aligned}
\Delta\boldsymbol{\delta}_{com} &= \frac{\partial}{\partial \boldsymbol{x}}\left(L_{G_1} L_{F_1} \boldsymbol{h}_1(\boldsymbol{x})\right)^{-1} \\
&\quad \left(\boldsymbol{v}(\boldsymbol{y}_{com}, \boldsymbol{x}) - L_{F_1}^2 \boldsymbol{h}_1(\boldsymbol{x})\right)\Big|_{\substack{\boldsymbol{x}=\boldsymbol{x}_0 \\ \boldsymbol{y}_{com}=\boldsymbol{y}_{com_0}}} \Delta\boldsymbol{x} \\
&+ \frac{\partial}{\partial \boldsymbol{y}_{com}}\left(L_{G_1} L_{F_1} \boldsymbol{h}_1(\boldsymbol{x})\right)^{-1} \\
&\quad \left(\boldsymbol{v}(\boldsymbol{y}_{com}, \boldsymbol{x}) - L_{F_1}^2 \boldsymbol{h}_1(\boldsymbol{x})\right)\Big|_{\substack{\boldsymbol{x}=\boldsymbol{x}_0 \\ \boldsymbol{y}_{com}=\boldsymbol{y}_{com_0}}} \Delta\boldsymbol{y}_{com} \\
&= \boldsymbol{K}_{\boldsymbol{y}_{com}}(\boldsymbol{x}_0, \boldsymbol{y}_{com_0})\Delta\boldsymbol{y}_{com} \\
&\quad - \boldsymbol{K}_{\boldsymbol{x}}(\boldsymbol{x}_0, \boldsymbol{y}_{com_0})\Delta\boldsymbol{x}
\end{aligned} \tag{42}$$

The closed and open loopsystem diagramsfor control surfaces are shown in Fig. 1 and Fig. 2 respectively. Indiagram (Fig. 2), it shows that the open loop system of aileron and other control surfaces (elevator and rudder) are still closed.

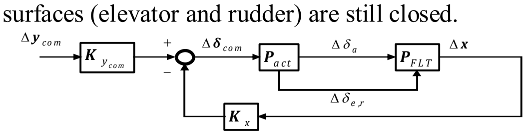

Fig. 1 Closed loop system

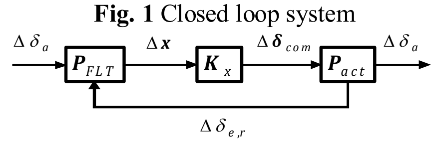

Fig. 2 Open loop system for aileron

Open loop system controller $\boldsymbol{K}_{\boldsymbol{x}}$ has a pseudo input vector, meaning the designer can tune the controller by changingdesired frequency. Generally, a damping ratio equal to $1/\sqrt{2}$ is acceptable, hence in this research, the authors tune only the desired frequency ($\omega_i\left(i = \alpha, \beta, \phi\right)$).

Similar to aircraft, winged rocket's stability can be evaluated by separating the dynamics into longitudinal dynamics and lateral-directional dynamics. From longitudinal dynamics, open loop transfer function for elevator is shown in(43). From lateral-directional dynamics, the transfer function for aileronand rudder are expressed in (44) and (45), respectively

$$L_{\delta_e/\delta_e}(s) = P_{act}\boldsymbol{K}_{\boldsymbol{x}_{Lon}}\boldsymbol{P}_{FLT_{Lon}} \tag{43}$$

$$L_{\delta_a/\delta_a}(s) = P_{act}\boldsymbol{K}_{\boldsymbol{x}_{Lat,Ail}}\Big\{ \boldsymbol{P}_{FLT_{Lat,Ail}} + \boldsymbol{P}_{FLT_{Lat,Rud}}\Big(1 - P_{act}\boldsymbol{K}_{\boldsymbol{x}_{Lat,Rud}}\boldsymbol{P}_{FLT_{Lat,Rud}}\Big)^{-1} P_{act}\boldsymbol{K}_{\boldsymbol{x}_{Lat,Rud}}\boldsymbol{P}_{FLT_{Lat,Ail}}\Big\} \tag{44}$$

$$L_{\delta_r/\delta_r}(s) = P_{act}\boldsymbol{K}_{\boldsymbol{x}_{Lat,Rud}}\Big\{ \boldsymbol{P}_{FLT_{Lat,Rud}} + \boldsymbol{P}_{FLT_{Lat,Ail}}\Big(1 - P_{act}\boldsymbol{K}_{\boldsymbol{x}_{Lat,Ail}}\boldsymbol{P}_{FLT_{Lat,Ail}}\Big)^{-1} P_{act}\boldsymbol{K}_{\boldsymbol{x}_{Lat,Ail}}\boldsymbol{P}_{FLT_{Lat,Rud}}\Big\} \tag{45}$$

where $\boldsymbol{P}_{FLT_i}$ is separated by locally linearized flight dynamics, subscript "Lon" means longitudinal dynamics, "Lat" means lateral-directional dynamics. $\boldsymbol{K}_{\boldsymbol{x}_i}$ is separated by locally linearized controller (subscripts are same as flight dynamics). About $\boldsymbol{P}_{FLT_{Lat}}$ and $\boldsymbol{K}_{\boldsymbol{x}_{Lat}}$,

$$\boldsymbol{P}_{FLT_{Lat}}(s) = \begin{bmatrix} \boldsymbol{P}_{FLT_{Lat,Ail}}(s) \\ \boldsymbol{P}_{FLT_{Lat,Rud}}(s) \end{bmatrix}^T \qquad \boldsymbol{K}_{\boldsymbol{x}_{Lat}} = \begin{bmatrix} \boldsymbol{K}_{\boldsymbol{x}_{Lat,Ail}} & \boldsymbol{K}_{\boldsymbol{x}_{Lat,Rud}} \end{bmatrix}^T \tag{46}$$

We can express $\boldsymbol{K}_{\boldsymbol{x}}$ as a function of desired frequency.

4.4 Desired frequency tuning algorithm

From (29), the condition for guaranteeing stability margin requirements is as following.

$$\max_{\omega} E_{k/k}(j\omega) \geq \frac{1}{R_{des}}\left(k = \delta_a, \delta_r, \delta_r\right) . \qquad E_{k/k}(j\omega) = \left(L_{k/k}(j\omega) + c_{des}\right)^{-1} \tag{47}$$

we need to define the circle condition from desired stability margins requirement. Second, select the desired frequency.Third, search the frequency ω where the evaluation function $E_{k/k}(j\omega)$ is maximum, and this frequency is expressed by ω_{peak}. If (47) is satisfied, desired frequency is defined. If (47) is not satisfied, back to second procedure. The detailed flowchart of this algorithm is shown in Fig. 3.In order to reduce the computing cost, this algorithm does not derive the exact peak gain of evaluation function, it selects a pseudo peak gain from the gains calculated by prepared candidate peak gain frequencies ($\omega_{peak,cand}$).The actuator response has to be faster than the closed loop response enough to approximate by linear transfer function. From this, we can specify the closed loop system response and this is an advantage of hierarchal dynamic inversion.

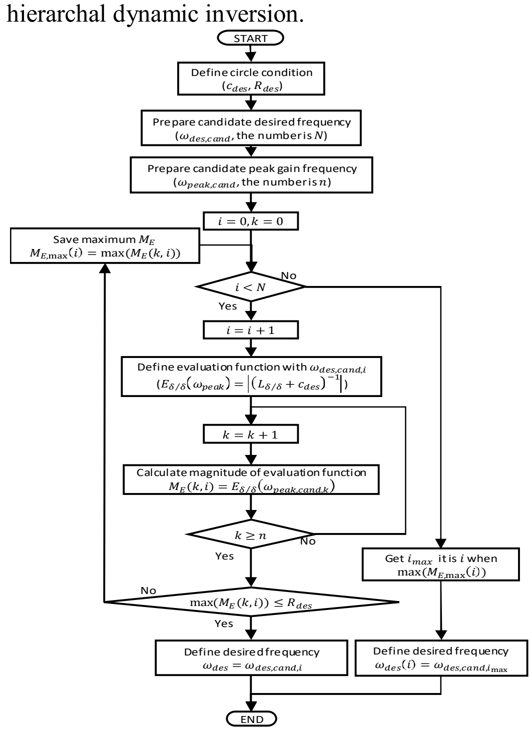

Fig. 3 Frequency Tuning algorithm

4.5 Numerical example

This section shows a result of numerical flight simulation where the desired frequency tuning algorithm is applied. In this section, it tunes the desired frequency of longitudinal dynamics and lateral-directional dynamics. It means $\omega_{Lon} = \omega_\alpha$ and $\omega_{Lat} = \omega_\beta = \omega_\phi$ are tuned. Bytuning ω_{Lat}, the condition of definition of desired frequency is that both of open loop system at aileron and rudder should satisfy (47). Simulation conditions are shown in Table 3-Table 7.

Table 3 WIRES vehicle specification

Body length	l_b	[m]	4.0
Mass	m	[kg]	672
Meanaerodynamic chord	c_{mac}	[m]	1.072
Wing Span	b	[rad/s]	2.88

Table 4 Initial condition

Altitude	20	[km]
Angle of attack	5	[deg.]
Mach number	0.27	[-]
True air speed	80	[m/s]
Pitch angle	0	[deg.]

Table 5 Control surface actuators specification

Characteristic frequency	f_{act}	[Hz]	4.0
	ω_{act}	[rad/s]	25.1 $\left(=2\pi f_{act}\right)$
Damping ratio	ζ_{act}	[-]	$1/\sqrt{2}$

Table 6 Candidate of desired frequencies and peak gain frequencies

Desired freq.	$\omega_{des,cand}=2\pi f_{des,cand}$	[rad/s]
	$f_{des,cand}=0.70,0.65,...,0.30$	[Hz]
Peak gain freq.	$\omega_{peak,cand}=2\pi f_{peak,cand}$	[rad/s]
	$f_{peak,cand}=1.0,1.1,...,3.($	[Hz]

Table 7 Stability margins requirement

Gain margin	6	[dB]
Phase margin	45	[deg.]

The results of the simulations are shown in Figs. 9 – 17..

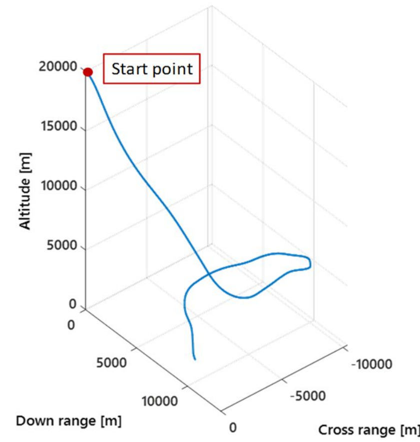

Fig. 4 Flight trajectory

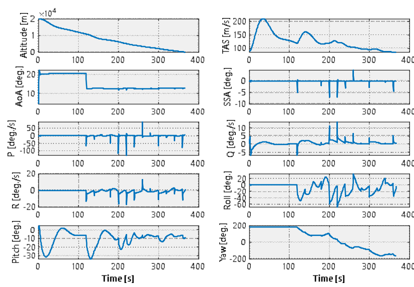

Fig. 5 Simulation result time history

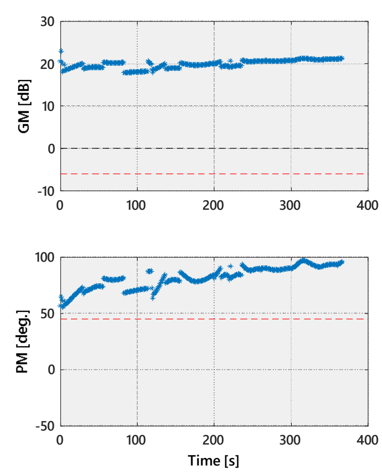

a) Aileron

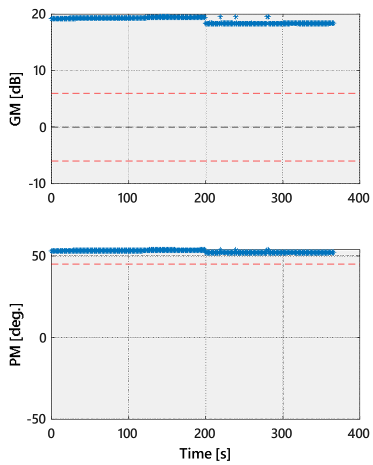

b) Elevator

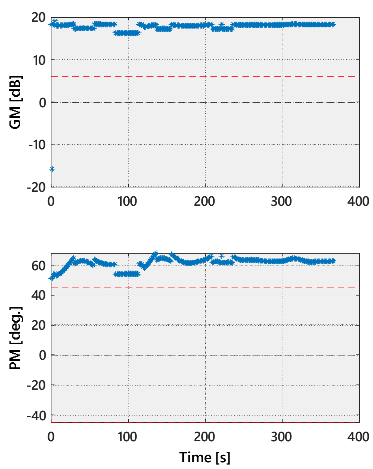

c) Rudder

Fig. 6 Stability margins time history

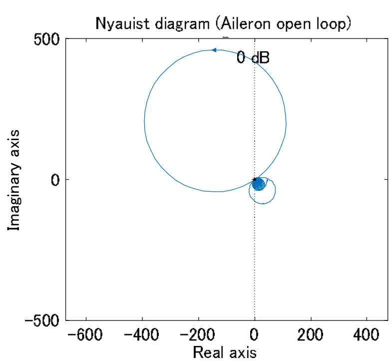

a) Aileron

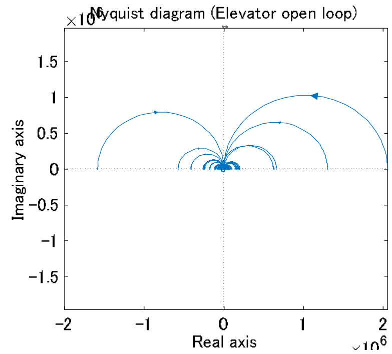

b) Elevator

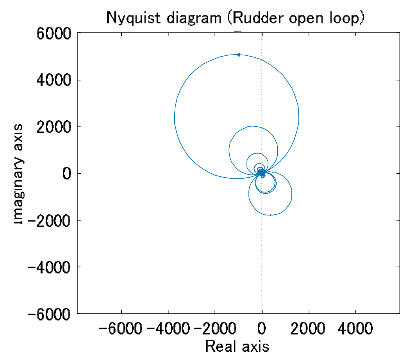

c) Rudder

Fig. 7 Nyquist diagram

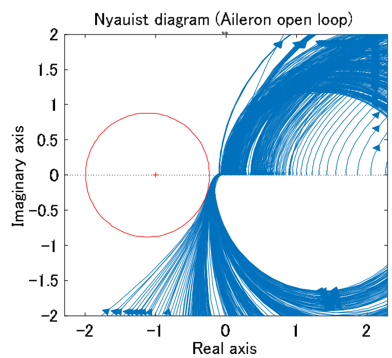

a) Aileron

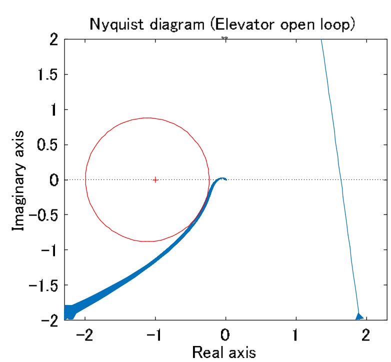

b) Elevator

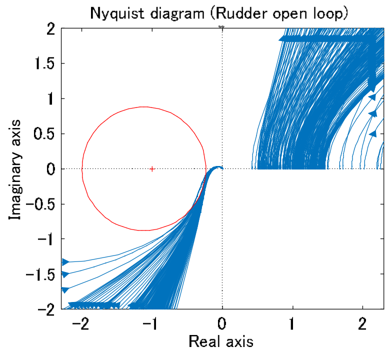

c) Rudder

Fig. 8 Nyquist diagram zoom on (-1,0)

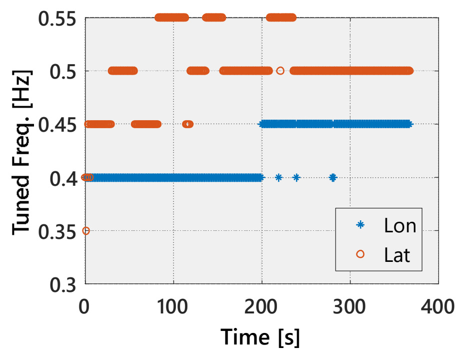

Fig. 9 Tuning result of desired frequencies

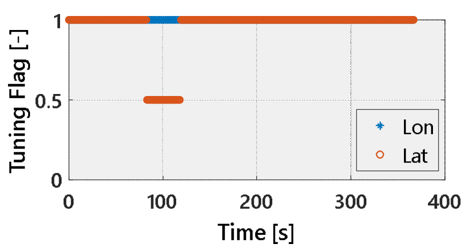

Fig. 10 Tuning successful

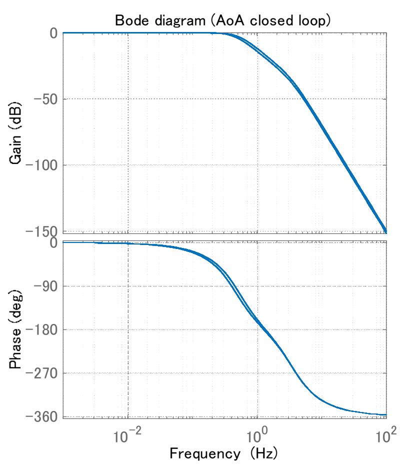

a) Angle of attack

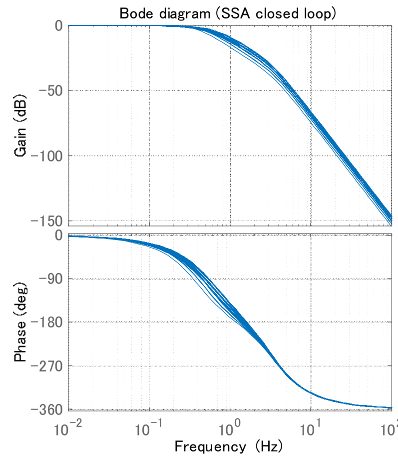

b) Side slip angle

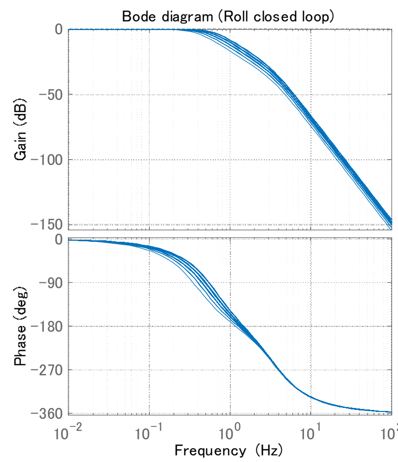

c) Roll angle

Fig. 11 Closed loop system

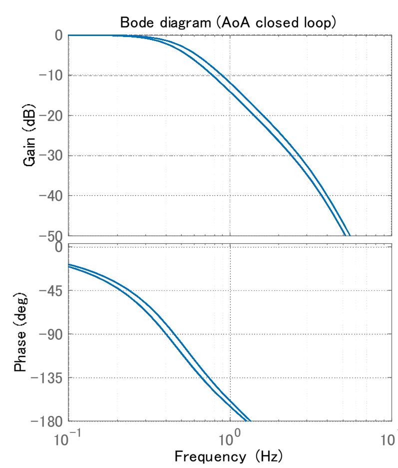

a) Angle of attack

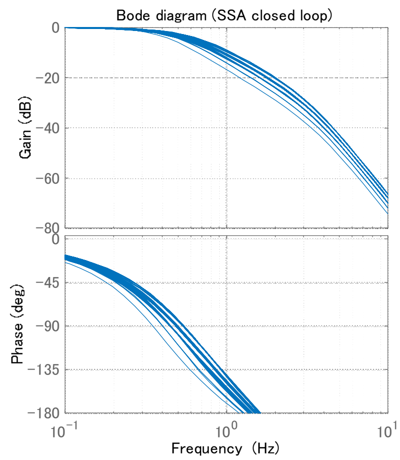

b) Side slip angle

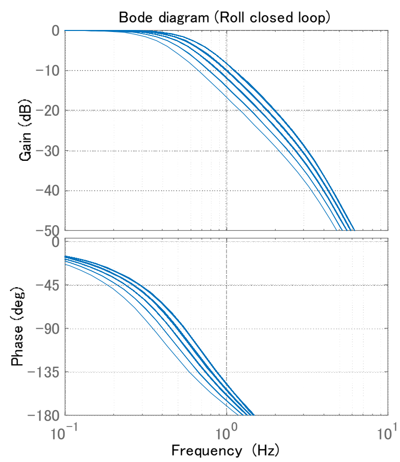

c) Roll angle

Fig. 12 Closed loop system (zoomed)

From Fig. 8, almost all Nyquist diagrams do not enter the circle condition. It means the distance between open loop system and designed center $\left(-c_{des}, 0\right)$ is always larger than R_{des} , thus the system satisfies the desired stability margins in this flight simulation. Fig. 11 also shows theabsolute value of margins are larger than desired margins.

From Fig. 17, AoA responses can be divided into two groups and SSA and roll responses can be divided into five groups. Thisis because the tuned desired AoA frequencies become 0.40 or 0.45 Hzand SSA and roll frequencies become 0.35, 0.40, 0.45, 0.50, or 0.55 Hz.

V. CONCLUSION AND FUTURE WORKS

In the first half of the article, the authors introduced a hierarchal dynamic inversion theory and gain tuning method for guaranteeing stability margins. In the latter half, the authors explained the gain tuning method for winged rocket attitude control system using DI. Also, a numerical example by flight simulation is shownand the proposed desired tuning method satisfies the stability margins (Fig. 11). However, sometimes it has failed the tuning frequencies. The possible reason can be assumed that the lateral-directional ideal frequencies are same.

The frequency tuning algorithm adjusted the desired frequency by choosing the appropriate one from candidate of desired frequency. Therefore, adjusted desired frequency is not an optimized result.Even if the desired frequencies changes, it is an advantage of hierarchal DI that the closed loop responses are known by the desired frequency and actuator dynamics without flight dynamics (flight state space).Therefore, desired closed loop response and stability margins are satisfied when the proposed method is used.

Currently the authors plan to study onthe following issues to improve the proposed method.

1. Upgrading the tuning algorithm with assumption that lateral-directional ideal frequencies are not necessary equal.
2. Optimization of desired frequency.

REFERENCES

[1]. A. Isidori, Nonlinear Control Systems (Berlin, Heidelberg, Springer-Verlag 1995) 145-172.

[2]. Y. Ochi, and K. Kanai, Design of Restructurable Flight Control Systems Using Feedback Linearization, Journal of Guidance, Control, and Dynamics, 14 (5), 1991, 903-911

[3]. P. K. A. Menon, V.R. Iragavarapu, E.J. Ohlmeyer, Nonlinear Missile Autopilot Design Using Time-Scale Separation, Proceeding of the AIAA Guidance, Navigation, and Control Conference, A I AA, New Orleans, Los Angles, 1997, 1791-1803

[4]. T. Ninomiya, H. Suzuki, and J. Kawaguchi, Evaluation of Guidance and Control System of D-SEND#2, IFAC-Papers Online, 49 (17), 2016, 106-111

[5]. T. Shimozawa, T. Narumi, S. Sagara, and K. Yonemoto, Digital Adaptive Control of Winged Rocket Using Unscented Kalman Filter, Artificial Life and Robotics, 16 (3) 2011,348-351

[6]. H. Yamasaki, K. Yonemoto, and T. Fujikawa, Stability Analysis of Nonlinear Control using Hierarchical Dynamic Inversion for a Winged Rocket, International Journal of Advanced Research,5 (10),2017, 200-218

[7]. O. Arrieta and R. Vianova, Simple PID tuning rules with guaranteed Ms robustness achievement, IFAC World Congress Milano, 18 (1), 2011, 12042-12047

[8]. V. M. Alfaro and R. Vianova, Model-reference robust tuning of 2 DoF PI

controllers for first-and second-order plus dead-time controlled processes, Journal of Process Control 22 (2), 2012, 359-374.

[9]. O. Arrieta and R. Vianova, J. D. Rojas, M. Meneses, Improved PID controller tuning rules for performance degradation/robustness increase trade-off, Electrical Engineering, 98 (3), 2016, 233-243

[10]. Y.B. Tossi, A Note of the Gain and Phase Margin Consepts, Journal of Control and Systems Engineering, 3 (1), 2015, 51-59

[11]. G. S. Gossamsetti, et al, Recent Development of Flight Demonstrators for Reusable Suborbital Technologies and it's Application, International Astronautical Congress (IAC 2018), Bremen, Germany, 2018

[12]. K. Yonemoto, et al., Subscale Winged Rocket Development and Application to Future Reusable Space Transportation, INCAS BULLETN, 10 (1), 2018,.161-172

[13]. K. Shirakata, et al., Development of Hardware-in-the-Loop Simulator for Experimental Winged Rocket, Asia-Pacific International Symposium on Aerospace Technology (APISAT2015), Cairns, Australia, 2015,.114-121

[14]. T. R. Yechout, et al., Introduction to Aircraft Flight Mechanics: Performance, Static Stability, Dynamic Stability, and Classical Feedback Control, (New York, U.S.A., American Institute of Aeronautics and Astronautics, 2003)

Kento Shirakata" Flight Attitude Controller Using Dynamic Inversion Theory with Stability Margin Guarantee' International Journal of Engineering Research and Applications (IJERA) , vol. 8, no.12, 2018, pp 16-27